PHILOSOPHICAL TRANSACTIONS OF THE ROYAL SOCIETY A MATHEMATICAL, PHYSICAL & ENGINEERING SCIENCES

Excitability, Wave Reflection, and Wave Splitting in a Cubic Autocatalysis Reaction-Diffusion System

Valery Petrov, Stephen K. Scott and Kenneth Showalter

Phil. Trans. R. Soc. Lond. A 1994 **347**, 631-642
doi: 10.1098/rsta.1994.0071

Excitability, wave reflection, and wave splitting in a cubic autocatalysis reaction-diffusion system†

By Valery Petrov[1], Stephen K. Scott[2] and Kenneth Showalter[1]

[1]*Department of Chemistry, West Virginia University, Morgantown, West Virginia 26506, U.S.A.*

[2]*School of Chemistry, University of Leeds, Leeds LS2 9JT, U.K.*

The excitability properties of a two-variable cubic autocatalysis model for chemical oscillations are examined. The reaction-diffusion behaviour of this model is studied in a one-dimensional configuration with differing relative diffusivities of the species. Wave reflection at no-flux boundaries is examined and described in terms of reactant depletion in the wave front and reactant influx in the wave back. Waves are also reflected upon collision with other waves. Wave splitting, the spontaneous initiation of a wave from the trailing edge of another wave, is found to occur for some relative diffusivities. Successive wave splittings give rise to stationary Turing patterns at long times.

1. Introduction

Excitable chemical and biological systems are often described in terms of minimal two-variable models. The two variables typically evolve on markedly different characteristic timescales, giving rise to a fast 'propagator' or 'trigger' variable and a slow 'controller' or 'recovery' variable (Winfree 1980; Murray 1989; Field & Burger 1985). In the Belousov–Zhabotinsky (BZ) reaction, the former role is played by bromous acid, $HBrO_2$, while the latter is played by the oxidized form of the metal-ion catalyst; in a nerve axon, the respective roles are played by the membrane potential and the ionic conductance. Such systems also display a typical structure in the two-dimensional phase plane (Winfree 1980; Tyson & Fife 1980). The fast variable has a folded nullcline consisting of three branches demarked by a maximum and a minimum in the locus. The slow motions of the system correspond to evolution along the outermost branches of this nullcline (the slow manifold), while the fast motions correspond to jumps from one branch to another as the system reaches either of the turning points. Excitability arises in such cases when there is a single intersection of the folded nullcline with the nullcline for the slow variable, and this intersection point lies close to the turning point on one of the stable (outer) branches. In this way, the system has local stability to sufficiently small perturbations, which decay directly back

† This paper was produced from the authors' disk by using the TEX typesetting system.

Phil. Trans. R. Soc. Lond. A (1994) **347**, 631–642
Printed in Great Britain

to the steady-state intersection point. Larger perturbations that exceed a critical threshold give rise to a single pulse of excitation as the system jumps across the phase plane to the other stable branch of the slow manifold. The system then evolves along this branch to its turning point, jumps back to the original branch and slowly moves toward the nullcline intersection to recover its steady state composition. The trajectory in the phase plane traces out an 'excitation cycle,' which is much like the limit cycle traced out when the nullcline of the slow variable intersects the middle branch of the folded nullcline (Dolnik *et al.* 1989, 1992). During a significant part of the traverse the system is refractory to further perturbations; however, its excitability is regained as the steady state is approached. In well-stirred, homogeneous systems, the excitation threshold is defined by the unstable (middle) branch of the slow manifold.

In this paper, we examine excitability arising in a different type of system. Multiple steady-state intersections exist, and the system is not easily split into fast and slow variables, as each variable has periods of acting in each role.

The model is that of cubic autocatalysis, which has been extensively studied in other configurations elsewhere (Gray & Scott 1984, 1990). We begin by revealing the characteristic features of excitability in this system under well-stirred conditions in a flow reactor (a CSTR), highlighting the differences and similarities to the classical scenario described above. We then examine the response of a reaction-diffusion system based on this model under parameter conditions for excitability appropriate to a continuously fed unstirred reactor (CFUR). We reveal the existence of wave reflection and spontaneous wave splitting in one spatial dimension. Such behaviour is dependent on the relative diffusivities of the variable species, and we examine this dependence. Our study is complementary to studies of wave reflection in a one-dimensional configuration by Röhricht & Horsthemke (1991) and of self-replicating spots in a two-dimensional configuration by Pearson (1993).

2. Model equations and parameter values

The cubic autocatalysis model of chemical feedback can be represented in the form,

$$\mathrm{A} + 2\mathrm{B} \rightarrow 3\mathrm{B}, \qquad \text{rate} = k_1 a b^2, \tag{2.1}$$

where A is a reactant species, B the autocatalyst, and a and b the respective concentrations. The rate constant for the process is k_1. We combine the autocatalytic step with a simple first-order decay of the autocatalyst:

$$\mathrm{B} \rightarrow \mathrm{C}, \qquad \text{rate} = k_2 b, \tag{2.2}$$

where k_2 is the rate constant for this step.

We imagine these two reactions taking place in a well-stirred tank reactor, continuously fed by inflow streams of both A and B. The mass-balance equations governing the rates of change of the two concentrations within the reactor can then be written in the form,

$$\frac{\mathrm{d}a}{\mathrm{d}t} = \frac{(a_0 - a)}{t_{\mathrm{res}}} - k_1 a b^2, \qquad \frac{\mathrm{d}b}{\mathrm{d}t} = \frac{(b_0 - b)}{t_{\mathrm{res}}} + k_1 a b^2 - k_2 b. \tag{2.3}$$

Here, a_0 and b_0 are related to the inflow concentrations of the reactant and autocatalyst and are the concentrations of these two species that would be established

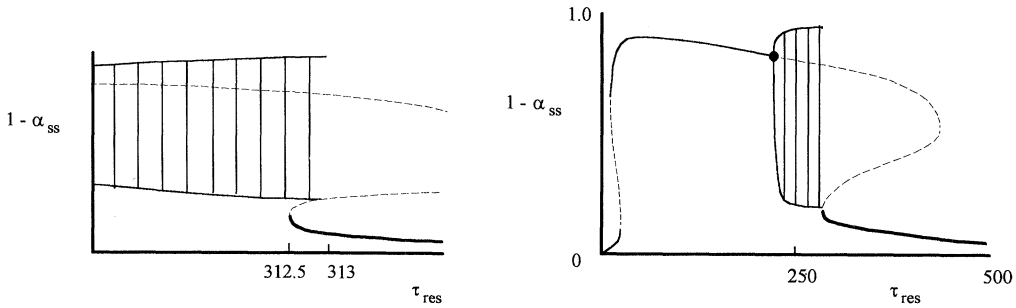

Figure 1. Bifurcation diagram showing steady-state extent of conversion $\gamma_{ss} = 1 - \alpha_{ss}$ as a function of residence time τ_{res}. Fixed parameter values $\beta_0 = \frac{1}{15}$ and $\kappa_2 = \frac{1}{40}$. Figure adapted from Gray & Scott (1984).

in the reactor in the absence of any reaction (allowing for the dilution of separate inflow streams). The mean residence time t_{res} is the ratio of the reactor volume and the total volumetric flow rate.

Equations (2.3) can be recast in dimensionless form, introducing $\alpha = a/a_0$, $\beta = b/a_0$, $\beta_0 = b_0/a_0$, $\tau = k_1 a_0^2 t$, $\tau_{res} = k_1 a_0^2 t_{res}$ and $\kappa_2 = k_2/k_1 a_0^2$ to give

$$\frac{d\alpha}{d\tau} = \frac{(1-\alpha)}{\tau_{res}} - \alpha\beta^2, \qquad \frac{d\beta}{d\tau} = \frac{(\beta_0 - \beta)}{\tau_{res}} + \alpha\beta^2 - \kappa_2\beta. \tag{2.4}$$

(*a*) *Parameter values and bifurcation diagram*

We will concentrate on the behaviour of this system for the specific parameter values $\beta_0 = \frac{1}{15}$ and $\kappa_2 = \frac{1}{40}$. The corresponding steady-state bifurcation diagram observed as the remaining parameter τ_{res} is varied has been determined elsewhere (Gray & Scott 1984) and is reproduced in figure 1. The steady-state locus describes a 'mushroom' pattern, with two ranges of multiple steady states, one at low τ_{res} and one at high τ_{res}. Additionally, there is a point of Hopf bifurcation along the uppermost branch of the mushroom, with the steady state losing stability and a stable limit cycle emerging as the residence time is increased. The locus of limit cycle solutions terminates at higher τ_{res} through the formation of a homoclinic orbit. (We have not determined precisely whether the orbit is formed to a regular saddle point or to the saddle-node point at the very edge of the region of multiple steady states, as this is not of particular relevance to the present study.) More importantly, for a range of τ_{res} beginning at 313, the system has three steady state solutions of which two are unstable (the saddle point on the middle branch and the unstable focus corresponding to the uppermost branch of the mushroom). The third steady state, corresponding to low extents of conversion (or high values of α), on the lowest branch of the mushroom is stable in this region. The stable steady state and the saddle point lie close together in the α–β phase plane provided τ_{res} is not much greater than 313. The phase plane structure for $\tau_{res} = 315$ is shown in figure 2*a*. Also shown are the two nullclines along which $d\alpha/d\tau = 0$ and $d\beta/d\tau = 0$, respectively, and the insets and outsets to the saddle point (see detail in figure 2*b*). The insets to the saddle play a vital role in determining the response of the system to perturbations away from the stable steady state.

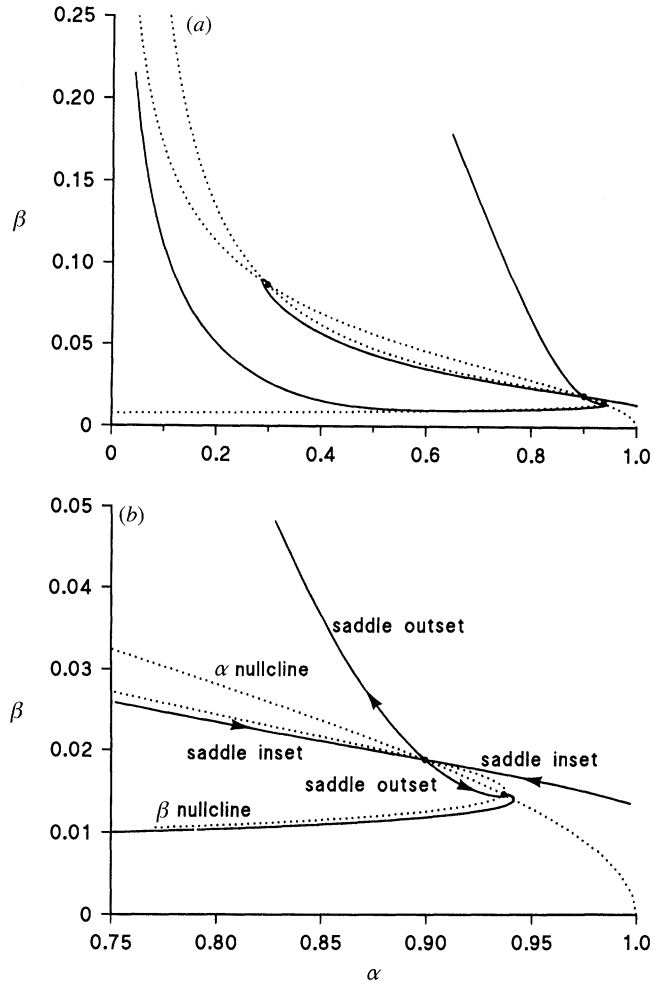

Figure 2. Phase plane for $\tau_{\mathrm{res}} = 315$. (*a*) Solid curves show inset and outset of saddle point; dotted curves show nullclines along which $\mathrm{d}\alpha/\mathrm{d}\tau = 0$ and $\mathrm{d}\beta/\mathrm{d}\tau = 0$. (*b*) Detail of region near saddle point and stable steady state (a stable node).

(*b*) *Excitability*

We now consider the response of a system, initially at the stable steady state, to small perturbations in the concentration of the autocatalyst concentration β. As shown in figure 3, if β is perturbed to the value 0.016, the response is a simple, direct return to the steady state. A similar response occurs when β is perturbed to 0.017. If, however, β is increased to 0.018, across the local path of the inset to the saddle point, the response is different. There is now a divergence from the vicinity of the stable steady state. A single large peak in the autocatalyst concentration and a corresponding trough in the reactant concentration is observed, shown in figure 4*a*, *b*, before the system recovers to its initial state, the stable steady state. The trajectory resulting from this supra-threshold perturbation traces out an 'excitation cycle' in the phase plane.

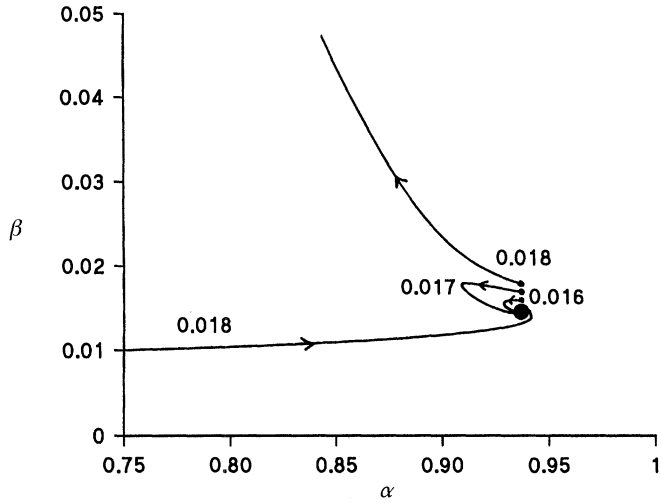

Figure 3. Response of system to perturbations in β. When β is perturbed to the value 0.016 or 0.017, the system returns directly to the steady state. When β is increased to 0.018, the response is a divergence from the vicinity of the stable steady state.

The relation between the excitation cycle trajectory and the α- and β-nullclines can be seen in figure 5. There is an initial fast motion which approximates the straight line $\beta = 0.73 - 0.83\alpha$ as α decreases. The peak in β occurs as the trajectory crosses the β-nullcline. This is followed by a period of relative slow motion along a segment of the α-nullcline as β varies from approximately 0.6 to 0.3. There is then motion corresponding to a transition from one nullcline to the other along which the product $\alpha\beta$ is approximately constant and equal to the value of κ_2. The final approach to the steady state closely follows the β-nullcline and the outset of the saddle point, which lie close together in this region of the phase plane. Therefore, the slow manifold is first comprised of a segment of one nullcline, while at a later stage it is comprised of the other nullcline.

3. Reaction-diffusion system

In the remainder of this paper, we will be concerned with the behaviour of the cubic autocatalysis model with parameter values the same as those discussed above, but now in a reaction-diffusion configuration. We begin with an effectively one-dimensional spatial domain over some range $0 \leqslant x \leqslant x_0$, where x is a dimensionless distance, with typically $x_0 = 3$. The governing reaction-diffusion equations have the form,

$$\frac{\partial \alpha}{\partial \tau} = \delta \nabla^2 \alpha + \frac{(1-\alpha)}{\tau_{\text{res}}} - \alpha\beta^2, \quad \frac{\partial \beta}{\mathrm{d}\tau} = \nabla^2 \beta + \frac{(\beta_0 - \beta)}{\tau_{\text{res}}} + \alpha\beta^2 - \kappa_2 \beta, \qquad (3.1)$$

with $\nabla^2 = \partial^2/\partial x^2$ in the one-dimensional case. Here, $\delta = D_{\text{A}}/D_{\text{B}}$ is the ratio of the diffusion coefficients of the reactant and autocatalyst. Typically, these may be of the same order of magnitude, but we are interested in the situation where they have significantly different values. Experimental methods are now known for selectively varying the effective diffusion coefficient for a given species in a reaction mixture (Lengyel & Epstein 1991, 1992).

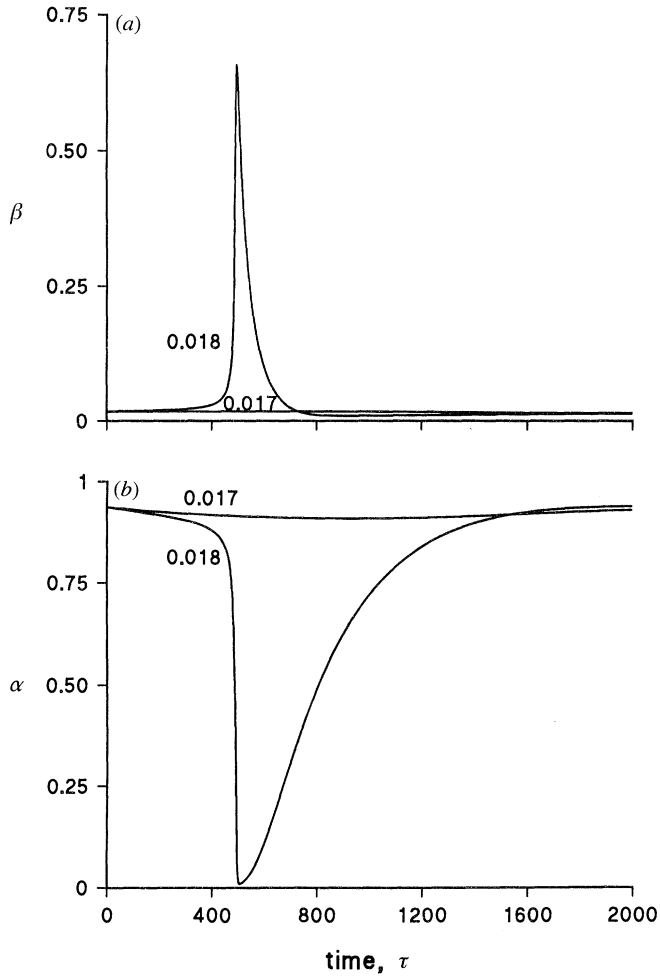

Figure 4. (a) Responses in β for perturbations to 0.017 and 0.018. (b) Corresponding responses in α.

We focus on the case where the diffusivity of the reactant is greater than that of the autocatalyst. Propagating fronts with cubic kinetics described by (2.1) have been previously considered in both one-dimensional and two-dimensional configurations (Hanna *et al.* 1982; Saul & Showalter 1985; Gray *et al.* 1987, 1991; Scott & Showalter 1992; Horváth *et al.* 1993). The two-dimensional fronts display instabilities for values of δ above a critical value of approximately 2.9, where the planar front gives way to various patterned fronts (Horváth *et al.* 1993). These isothermal fronts are much like non-isothermal flame fronts (Sivashinsky 1977, 1983, 1990), and δ is analogous to the Lewis number, Le. In both the isothermal and non-isothermal cases, the planar front is replaced by steady non-planar fronts on increasing the value of δ or Le; these, in turn, lose their temporal stability. The spatiotemporal behaviour includes oscillations of the various non-planar waveforms, including period-doubling cascades to chaos. A similar difference in diffusivities gives rise to Turing patterns in reaction-diffusion systems such as

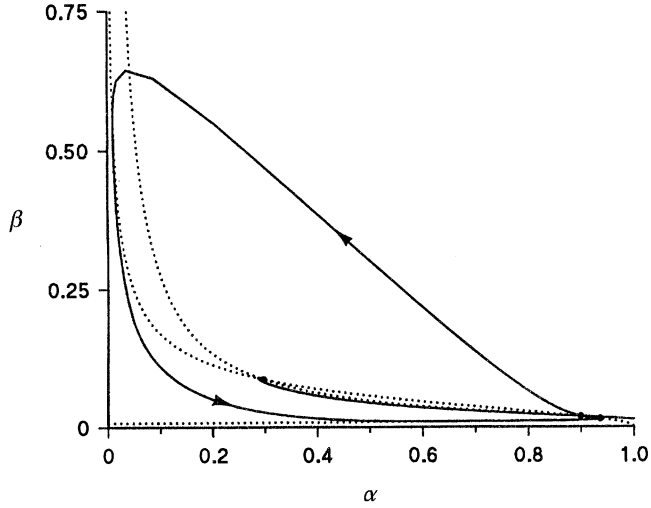

Figure 5. Trajectory of excitation cycle (solid line) resulting from supra-threshold perturbation in β. Also shown are saddle point (middle), unstable focus (left) and stable node (right). Dotted lines show the α and β nullclines; inset of the saddle point shown by solid lines.

(3.1), in which the reaction kinetics is oscillatory. Many theoretical studies of Turing patterns have been carried out (Turing 1952; Nicolis & Prigogine 1977; Haken 1977; Meinhardt 1986; Murray 1989; Dufiet & Boissonade 1992; Borckmans *et al.* 1992), and recently experimental examples of such patterns have been characterized (Castets *et al.* 1990; De Kepper *et al.* 1991; Ouyang & Swinney 1991*a*, *b*; Lengyel & Epstein 1992; Lengyel *et al.* 1992). A recent experimental study of pattern formation (Lee *et al.* 1993) appears to be closely related to the cubic autocatalysis model we consider here. These patterns have been modelled with (3.1) in a two-dimensional configuration by Pearson (1993).

(*a*) *Wave reflection*

The effects of a higher relative diffusivity of the reactant on wave propagation are shown in figure 6. The space-time plot shows the profile of β at equal increments of time, with time increasing from top to bottom. The wave propagates from right to left at the top of the figure. On approaching the boundary, it slows down, stops, and reverses its direction of propagation. Now propagating from left to right, the wave quickly attains a constant velocity, as shown by the positions of the maxima in β. On approaching the right-hand boundary, the wave again slows down and stops before reaching $x = 3.0$. It then propagates in the opposite direction, with its speed quickly increasing to a constant value. Wave reflection at no-flux boundaries has also been studied by Röhricht & Horsthemke (1991) using the cubic autocatalysis scheme.

Insights into the mechanism of wave reflection can be developed by examining the profiles of α and β as the wave approaches the boundary. Shown in figure 7*a* is a wave propagating from left to right, with α and β displaying sharp gradients in the leading edge and shallow gradients in the wave back. As the wave approaches the boundary, shown in figure 7*b*, the 'inflow' of the reactant A from the surroundings into the region ahead of the front cannot match its consumption (by diffusion into the reaction zone). The concentration α ahead of the front

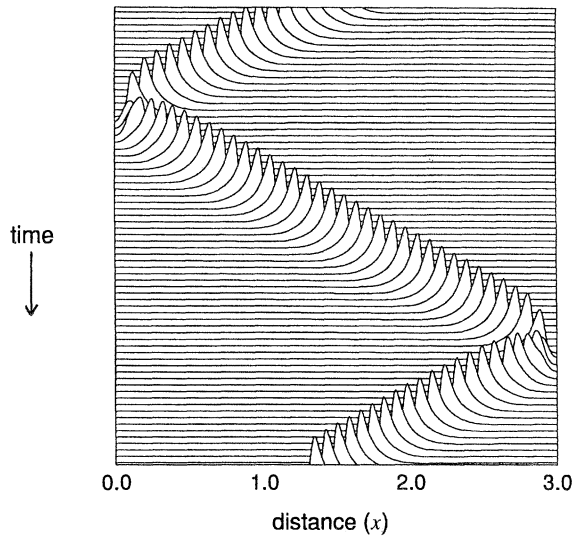

Figure 6. Space-time plot showing profiles of β in wave reflected at boundaries. Calculated from (3.1) using 300 grid points with $\delta = D_A/D_B = 7$ and $D_B = 1.0 \times 10^{-5}$ cm^2 s^{-1}. All distances were scaled by a factor of $(10^{-5})^{1/2}$. All other parameters same as in figures 2–5. Each profile corresponds to an increment of 100 dimensionless time units.

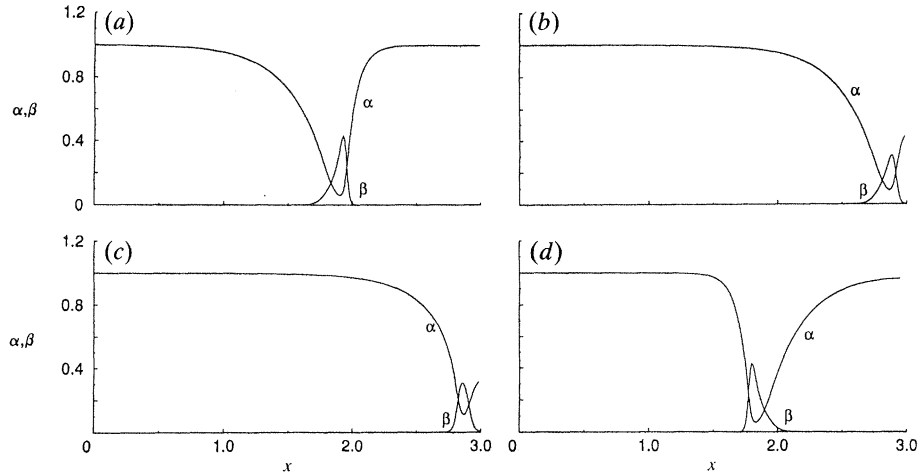

Figure 7. Profiles of α and β in wave reflected at boundary. (a) Wave propagating from left to right; (b) level of α is depleted between wave front and boundary; (c) profile of β becomes approximately symmetrical as propagation velocity reaches zero; (d) wave propagating from right to left. Parameters for calculation same as in figure 6.

decreases significantly, the maximum in β decreases and the gradient of α in the wave front becomes less sharp. The propagation velocity also decreases as the available reactant and extent of chemical reaction decrease. This trend continues with the wave velocity approaching zero, which coincides with the β profile becoming nearly symmetrical, as shown in figure 7c. At this point, the α gradient becomes steeper in the wave back than in the wave front due to the influx of reactant from the bulk. With the corresponding increase in reactant concentra-

PHILOSOPHICAL TRANSACTIONS OF THE ROYAL SOCIETY A MATHEMATICAL, PHYSICAL & ENGINEERING SCIENCES

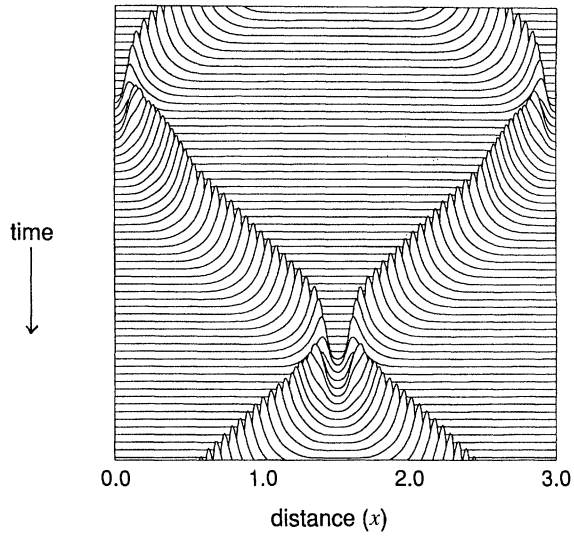

Figure 8. Space-time plot showing profiles of β in two waves reflected at boundaries and then from each other. Parameters same as in figure 6. Each profile corresponds to an increment of 40 dimensionless time units.

tion, the medium recovers sufficiently in the wave back to sustain a reaction event propagating in the opposite direction: the wave reverses its direction of propagation. Figure 7*d* shows the wave propagating from right to left, again with steep gradients in the wave front and relatively shallow gradients in the wave back.

Reactant depletion not only affects wave propagation near the boundary, but also when one wave meets another. Shown in figure 8 are two waves, which, after being reflected from the boundaries, propagate toward each other. Depletion of reactant becomes important as the waves draw closer to each other. Each wave slows down, stops and reverses its direction of propagation in the encounter. The space-time plot of this two-wave system shows periodic behaviour, with the waves reflected at the boundaries and from each other at regular time intervals. A slight oscillation in the maximum of β is exhibited following each reflection, which can be more easily seen in enlargements of figures 6 and 8.

The high diffusivity of the reactant plays a double role in the wave reflections. As a wave approaches a boundary or another wave, diffusion of reactant into the wave front and its consumption by chemical reaction causes its concentration to decrease in the region ahead of the wave. It is depleted at a greater rate than it can be replenished by the reactant inflow. Behind the wave, diffusion of reactant into the wave back provides for an increase in concentration, leading to a recovery of the 'excitability' of the system to further reaction events. Additional work by Winfree (A. T. Winfree 1993, personal communication) has shown that very similar responses are observed for parameter values, in particular for a lower value of τ_{res}, such that the system has only one (unstable) steady-state surrounded by a stable limit cycle: the phase-plane trajectory of the wave motion for the reaction-diffusion system is, however, quite different from the path described by the limit cycle for the corresponding well-stirred system in such cases.

PHILOSOPHICAL TRANSACTIONS OF THE ROYAL SOCIETY A MATHEMATICAL, PHYSICAL & ENGINEERING SCIENCES

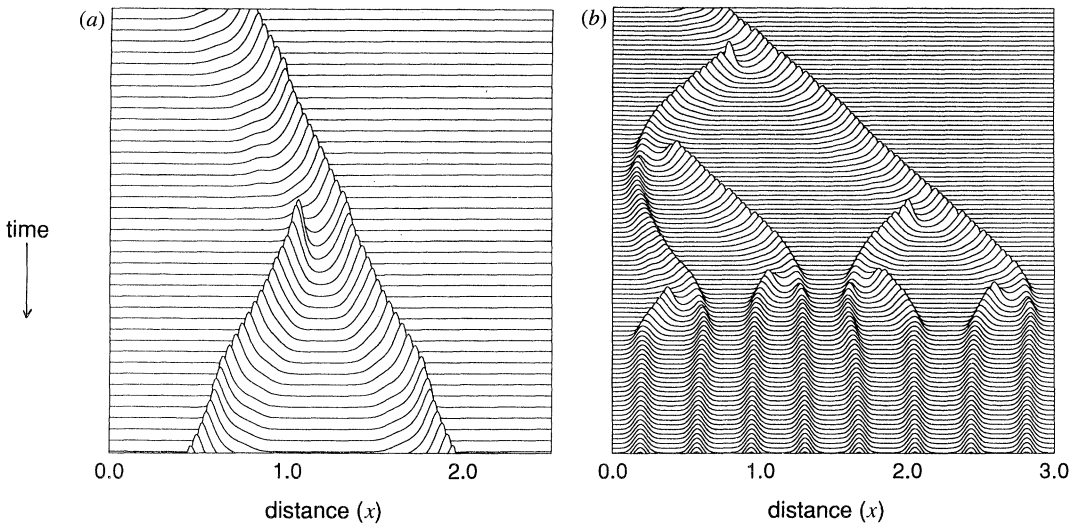

Figure 9. (*a*) Space-time plot showing profiles of β in wave splitting, giving rise to second wave propagating in other direction. Parameters same as in figure 6 except $\delta = 17$. Each profile corresponds to an increment of 20 dimensionless time units. (*b*) Long-time behaviour, with each profile corresponding to an increment of 60 dimensionless time units.

(*b*) *Wave splitting*

A new feature arises when the reactant diffusivity is further increased. As shown in figure 9, the medium may become unstable to spontaneous wave initiation in the wake of a wave. In this case, the reactant diffusivity has been increased such that $\delta = 17.0$. The high diffusivity of the reactant plays a similar role in the spontaneous wave initiations as in the wave reflections.

When the diffusivities of the reactant and autocatalyst are equal, the wave back is highly refractory (i.e. 'non-excitable'), since the reactant concentration is reduced to very low levels. The phase plane trajectory for the homogeneous system, shown in figure 5, is qualitatively similar to the trajectory for the reaction-diffusion system with $\delta = 1$ as a wave passes through a particular grid point. The refractory wave back occurs following the maximum in β, as the reactant is almost completely consumed and the value of α becomes very small. In the homogeneous system, the recovery of the reactant concentration occurs when the value of α increases due to the influx of reactant. In the reaction-diffusion system, diffusion of reactant into the wave back also plays a role in the recovery process. When the relative diffusivity of the reactant is increased, the region of the trajectory corresponding to the wave back is shifted to higher values of α due to the diffusive influx of reactant. Wave splitting occurs when the relative reactant diffusivity is so high that the wave back becomes 'excitable'.

The behaviour shown in figure 9*a* is only the initial stage in the evolution to an asymptotic pattern. Each newly created wave generates a new wave in its wake, until the medium is saturated with waves. As shown in figure 9*b*, the asymptotic state is a stationary Turing pattern. In the context of wave reflections and splittings, the Turing pattern arises because the medium becomes saturated with waves and each symmetrical wave is reflected from its neighbouring waves.

PHILOSOPHICAL TRANSACTIONS OF THE ROYAL SOCIETY A MATHEMATICAL, PHYSICAL & ENGINEERING SCIENCES

The balance of reactant inflow and its consumption by chemical reaction gives rise to waves that are locked into a time-independent pattern.

4. Conclusions

Many theoretical and experimental studies have been carried out on systems exhibiting the Turing instability. Recently, more attention has been paid to behaviour that lies between the regimes of stationary patterns and propagating waves. A recent report by Pearson (1993) showed that the same model considered here exhibits replicating spots in a two-dimensional spatial configuration. This behaviour is strikingly similar to that found in an experimental system by Swinney and co-workers (Lee *et al.* 1993). They studied the iodate–sulphite–ferrocyanide reaction in a CFUR and perturbed the photosensitive system with light to initiate pattern formation. The chemical mechanism of this reaction (Edblom *et al.* 1986; Gáspár & Showalter 1987, 1990) has many features in common with the cubic autocatalysis model (Gray & Scott 1984) used by Pearson and in this study. We have also carried out studies of a two-dimensional configuration and found virtually the same behaviour reported by Pearson. The wave splitting in one dimension and replicating spots in two dimensions are closely related and arise from excitability in the wave back due to high reactant diffusivity. Whether the simple cubic autocatalysis model is directly relevant to the experimental observations remains to be determined.

We thank the National Science Foundation (Grant no. CHE-9222616), the Fulbright Commission, NATO (Grant No. 0124/89) and WV-EPSCoR (Grant No. OSR-9255224) for supporting this research. Acknowledgment is made to the donors of The Petroleum Research Fund, administered by the ACS, for partial support of this research. We also thank Werner Horsthemke for providing a prepublication manuscript on studies of wave reflection and Art Winfree for stimulating discussion.

References

Borckmans, P., De Wit, A. & Dewel, G. 1992 *Physica* A **188**, 137.

Castets, V., Dulos, E., Boissonade, J. & De Kepper, P. 1990 *Phys. Rev. Lett.* **64**, 2953.

De Kepper, P., Castets, V., Dulos, E. & Boissonade, J. 1991 *Physica* D **49**, 161.

Dolnik, M., Finkeová, J., Schreiber, I. & Marek, M. 1989 *J. phys. Chem.* **93**, 2764.

Dolnik, M., Marek, M. & Epstein, I. R. 1992 *J. phys. Chem.* **96**, 3218.

Dufiet, V. & Boissonade, J. 1992 *J. chem. Phys.* **96**, 664.

Edblom, E. C., Orbán, M. & Epstein, I. R. 1986 *J. Am. chem. Soc.* **108**, 2826.

Field, R.J. & Burger, M. 1985 *Oscillations and traveling waves in chemical systems.* New York: Wiley.

Gáspár, V. & Showalter, K. 1987 *J. Am. chem. Soc.* **109**, 4869.

Gáspár, V. & Showalter, K. 1990 *J. phys. Chem.* **94**, 4973.

Gray, P. & Scott, S. K. 1984 *Chem. Engng Sci.* **39**, 1087.

Gray, P., Showalter, K. & Scott, S. K. 1987 *J. Chim. phys.* **84**, 1329.

Gray, P. & Scott, S. K. 1990 *Chemical oscillations and instabilities.* Oxford University Press.

Gray, P., Scott, S. K. & Showalter, K. 1991 *Phil. Trans. R. Soc. Lond.* A **331**, 249.

Haken, H. 1977 *Synergetics, an introduction.* Berlin: Springer-Verlag.

Hanna, A., Saul, A. & Showalter, K. 1982 *J. Am. chem. Soc.* **104**, 3838.

PHILOSOPHICAL TRANSACTIONS OF THE ROYAL SOCIETY A MATHEMATICAL, PHYSICAL & ENGINEERING SCIENCES

Horváth, D., Petrov, V., Scott, S. K. & Showalter, K. 1993 *J. chem. Phys.* **89**, 6332.
Lee, K. J., McCormick, W. D., Ouyang, Q. & Swinney, H. L. 1993 *Science, Wash.* **261**, 192.
Lengyel, I. & Epstein, I. R. 1991 *Science, Wash.* **251**, 650.
Lengyel, I. & Epstein, I. R. 1992 *Proc. natn. Acad. Sci. U.S.A.* **89**, 3977.
Lengyel, I., Kadar, S., & Epstein, I. R. 1992 *Phys. Rev. Lett.* **69**, 2729.
Meinhardt, H. 1986 *Models of biological pattern formation.* New York: Academic.
Murray, J. D. 1989 *Mathematical biology.* Berlin: Springer-Verlag.
Nicolis, G. & Prigogine, I. 1977 *Self-organization in nonequilibrium systems.* New York: Wiley.
Ouyang, Q. & Swinney, H. L. 1991*a* *Nature, Lond.* **352**, 610.
Ouyang, Q. & Swinney, H. L. 1991*b* *Chaos* **1**, 411.
Pearson, J. E. 1993 *Science, Wash.* **261**, 189.
Röhricht, B. & Horsthemke, W. 1991 Preprint.
Saul, A. & Showalter, K. 1985 In *Oscillations and traveling waves in chemical systems* (ed. R. J. Field & M. Burger), ch. 11, p. 419. New York: Wiley.
Scott, S. K. & Showalter, K. 1992 *J. phys. Chem.* **96**, 8702.
Sivashinsky, G. I. 1977 *Combust. Sci. Technol.* **15**, 137.
Sivashinsky, G. I. 1983 *A. Rev. Fluid. Mech.* **15**, 179.
Sivashinsky, G. I. 1990 *Phil. Trans. R. Soc. Lond.* A **332**, 135.
Turing, A. M. 1952 *Phil. Trans. R. Soc. Lond.* B **237**, 37.
Tyson, J. J. & Fife, P. C. 1980 *J. chem. Phys.* **73**, 2224.
Winfree, A. T. 1980 *The geometry of biological time.* Berlin: Springer.

PHILOSOPHICAL TRANSACTIONS OF THE ROYAL SOCIETY A MATHEMATICAL, PHYSICAL & ENGINEERING SCIENCES